




Internship report:

# Plaquette models for glasses

Stefano Spigler*

07 May 2014

*Supervisor:* Prof. Silvio Franz, LPTMS, Université Paris Sud XI

## Contents

**1 Introduction to plaquette models** **2**

**2 Incommensurable triangular plaquette model** **4**

**3 Random long range triangular plaquette model** **14**

**4 Bethe lattice approximation** **15**

**5 Conclusions** **21**

**6 Bibliography** **22**

*stefano@spigler.net

# 1 Introduction to plaquette models

Glassy dynamics can be found both in models with a complex energy landscape and hence a non-trivial thermodynamics (e.g. spherical $p$-spin model), or in models where the thermodynamics is trivial and the critical slowing down at low temperatures is only due to constraints in the rules of microscopic dynamics. In the former case, it is believed that glassiness is due to a large number of metastable states separated by barriers which increase as the temperature is lowered, eventually leading to a true ergodicity breaking transition (e.g. [2]). In the latter scenario, usually referred to as "dynamical facilitation" scenario, the system is governed by a dynamics where the allowed moves depend on the state of the neighboring variables (e.g. [5]): such dynamics can become exponentially slow when available moves are very rare, that is, when the density of "mobility defects" vanishes. These models are called Kinetically Constrained Models (KCMs) [7].

Plaquette models (PMs) are lattice models with plaquette ($p$-spin) interactions between neighboring Ising spin variables lying on the vertices. 1d Ising is the simplest PM, with 2-spins plaquettes; on a 2d square lattice, for instance, we can define a ferromagnetic interaction $-J\sum_{ij} s_{ij}s_{i+1j}s_{ij+1}s_{i+1j+1}$, and analogous definitions hold for any regular grid. In this report we only work on triangular lattices; they can have 3-spins interactions either on every triangle (made of neighboring spins) as in the Baxter-Wu model (BWM, [1]) or on upward-pointing triangles only as in the Newman-Moore model (NMM, [11]). The BWM does not exhibit glassy behavior, and thus we do not study it; on the other hand, the NMM is an integrable model which has a glassy behavior at low temperatures, namely the characteristic time $\tau$ of its relaxational dynamics grows with the super-Ahrrenius behavior $\tau \sim \exp(1/2 \log 2T^2)$.

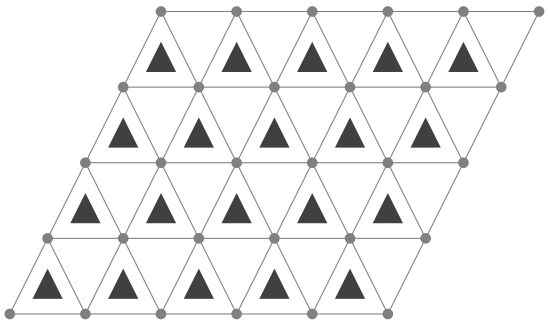

Figure 1: Triangular lattice for the Newman-Moore model. The interacting plaquettes are shown as dark gray triangles within the lattice cells.

The Hamiltonian of this model is

$$H_0 = -J \sum_{\triangle} s_{\triangle(1)} s_{\triangle(2)} s_{\triangle(3)} \equiv -J \sum_{\triangle} \sigma_{\triangle},$$

where $\sum_{\triangle}$ means that the sum is over all upward-pointing triangles and $s_{\triangle(i)}$ is a spin belonging to the triangle $\triangle$ (as shown in Fig. 1); the relationship between spin and plaquette variables is bijective (with suitable boundary conditions on the lattice size). What makes this model interesting is that the Hamiltonian is ordered, without any randomness or frustration, and with short-range interactions; furthermore, the statics is exactly solvable. At low temperature, this model can be described both as an interacting spin system and as a system governed by a constrained defect dynamics (in which 3 neighboring defects are flipped for a single spin flip, [6]). In terms of plaquette variables, the Hamiltonian is the same as that of a set of non-interacting spins in a magnetic field, and therefore the partition function is $Z = 2^N \cosh^N(\beta J)$, where $N$ is the number of such spins. Clearly this model has no finite temperature transition, with the only critical point $T = 0$; the purpose of our work is to find a perturbation of the Newman-Moore model which shifts the critical point at $T > 0$, while leaving almost unchanged the local dynamics of the model.

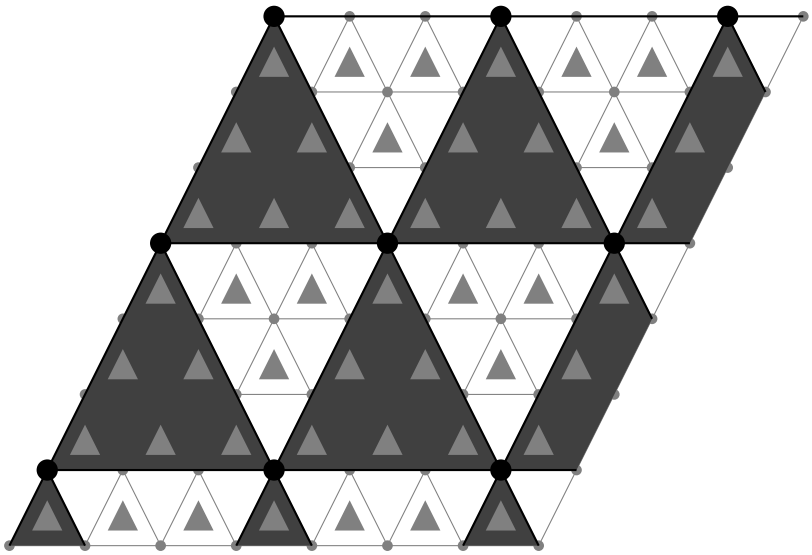

Figure 2: Triangular lattice for the generalized NM model. NM and additional interactions are shown as light gray and dark gray triangles, respectively.

## 2 Incommensurable triangular plaquette model

The first perturbation to the Newman-Moore model that we study is the addition of extra ferromagnetic (triangular) plaquette interactions, as shown in Fig. 2. Such interactions are of the form

$$H_1 = -J' \sum_{ij}{}' s_{ij} s_{i+3j} s_{ij+3} \equiv -J' \sum_{\text{⧋}} s_{\text{⧋}(1)} s_{\text{⧋}(2)} s_{\text{⧋}(3)} \equiv -J' \sum_{\text{⧋}} \sigma_{\text{⧋}}, \quad (1)$$

where $\sum'$ means that $(i,j) \in 3\mathbb{Z}^2$: the indices run on a sublattice whose cells are three times bigger than the NMM lattice. Each triplet of interacting spins in $H_1$, namely placed at the vertices of an upward-pointing triangle of this sublattice $3\mathbb{Z}^2$, in the following will be refered to as big plaquette (⧋).

In the beginning, in order to understand the relevance of the perturbation $H_1$, we attempted to prove that the high temperature expansion of the partition function $Z = \sum_{\{s\}} e^{H_0[\{s\}]+\varepsilon H_1[\{s\}]}$ was trivial (i.e. similar to the one of the NMM but with a different number of plaquettes, $Z_{HTE} = 2^N \cosh^{N+\frac{N}{6}}(\beta J)$, where $\frac{N}{6}$ is the number of big plaquettes); looking at the simulations this seemed to be the case. Unfortunately it is not true, and we will show why in what follows.

If we define $c = \cosh(\beta J), t = \tanh(\beta J)$ (in the following $\varepsilon J' = J$), the partition function $Z$ then reads

$$\begin{aligned} Z &= c^{N_{\text{⧋}}} \sum_{\{s\}} e^{\beta J \sum_{\triangle} \sigma_{\triangle}} \prod_{\text{⧋}} (1 + t\sigma_{\text{⧋}}) = \\ &= c^{N_{\text{⧋}}} \sum_{\{s\}} e^{\beta J \sum_{\triangle} \sigma_{\triangle}} \sum_{\mathcal{C}} t^{|\mathcal{C}|} \prod_{\text{⧋} \in \mathcal{C}} \sigma_{\text{⧋}} = \\ &= Z_{\triangle} c^{N_{\text{⧋}}} \sum_{\mathcal{C}} t^{|\mathcal{C}|} \left\langle \prod_{\text{⧋} \in \mathcal{C}} \sigma_{\text{⧋}} \right\rangle_{\triangle}, \end{aligned} \quad (2)$$

where $\langle \mathcal{O} \rangle_{\triangle} = Z_{\triangle}^{-1} \sum_{\{s\}} \mathcal{O} e^{\beta J \sum_{\triangle} \sigma_{\triangle}}$ and $\mathcal{C}$ ranges over all possible diagrams made of big plaquettes, and $|\mathcal{C}|$ is the number of big plaquettes in each diagram. Hence, to prove our thesis, we want to show that for every finite diagram $\mathcal{C}$ the correlation $\langle \prod_{\text{⧋} \in \mathcal{C}} \sigma_{\text{⧋}} \rangle_{\triangle}$ is zero: this is equivalent to say that within the expression $\prod_{\triangle}(1 + t\sigma_{\triangle}) \prod_{\text{⧋} \in \mathrm{C}} \sigma_{\text{⧋}}$ there is no closed diagram.

### Mapping to a XORSAT problem

It is worth noting that the conditions for the closure of the diagrams can be expressed as a XORSAT problem: such problem consists in assigning values to $N$ boolean variables such that they satisfy simultaneously $M$ linear equations modulo 2. The diagram $\prod_{\text{⧋} \in \mathcal{C}} \sigma_{\text{⧋}}$ can be closed if and

only if there exists at least one diagram $\mathcal{L}$ made of small plaquettes such that $\prod_{\triangle\in\mathcal{L}}\sigma_{\triangle}\prod_{\hexagon\in\mathcal{C}}\sigma_{\hexagon}=\prod_{\triangle\in\mathcal{L}}s_{\triangle(1)}s_{\triangle(2)}s_{\triangle(3)}\prod_{\hexagon\in\mathcal{C}}s_{\hexagon(1)}s_{\hexagon(2)}s_{\hexagon(3)}=1$, namely each spin appers an even number of times. For the sake of clarity let us define as $\mathcal{I}_{\mathcal{C}}$ the set of all spins appearing in $\prod_{\hexagon\in\mathcal{C}}s_{\hexagon(1)}s_{\hexagon(2)}s_{\hexagon(3)}$. Then, introducing the variables $n_{\triangle}$ which are set equal to 1 (0) if $\triangle\in\mathcal{L}$ ($\triangle\notin\mathcal{L}$) and $n_{\hexagon}$ which are set equal to 1 (0) if $\hexagon\in\mathcal{C}$ ($\hexagon\notin\mathcal{C}$), it is easy to show that the diagram $\mathcal{L}\cup\mathcal{C}$ is closed if and only if the following equation holds for any site $i$ of the lattice:

$$\sum_{\triangle\in\mathcal{L}\cap\partial i}n_{\triangle}+\sum_{\hexagon\in\mathcal{C}\cap\partial i}n_{\hexagon}\equiv 0\ (\mathrm{mod}\ 2),\tag{3}$$

where $\triangle\in\partial i$ means that $\triangle$ contains the spin in vertex $i$. In particular let us notice that for every spin $i\notin\mathcal{I}_{\mathcal{C}}$, we have $\sum_{\hexagon\in\mathcal{C}\cap\partial i}n_{\hexagon}\equiv 0\ (\mathrm{mod}\ 2)$. What (3) actually means is that, given a diagram $\mathcal{C}$ mqde of big plaquettes, it can be closed if and only if we can find a small plaquette diagram such that the total number of small and big plaquettes around each vertex is even. With the purpose of proving that this is never possible, we study a game in which the diagram $\mathcal{C}$ is given and the task is to find the values $\{n_{\triangle}\}$ that satisfy (3). As a first step, it can be shown that, on an infinite lattice (i.e. in the thermodynamic limit), $n_{\triangle}$ has to be 0 for each small plaquette outside a certain minimum hull containing the diagram $\mathcal{C}$ (this minimum hull in general has a strange shape, but it is always inside the minimal hexagonal hull containing $\mathcal{C}$).

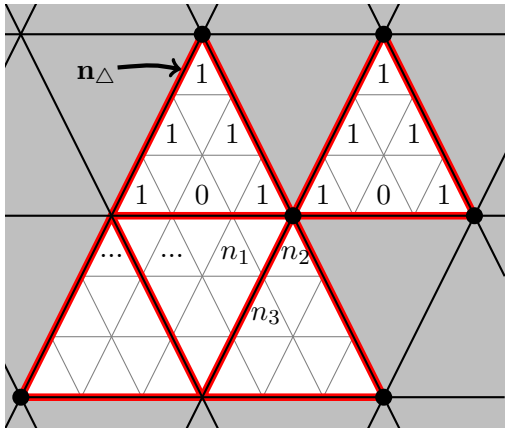


Figure 3: In this figure the set $\mathcal{C}$ is made by the four big plaquettes with thick red borders; note that the two middle vertices on the bottom and left borders have not been marked as the others, since, being a superposition of two "big plaquette vertices", it is not relevant for (3). The light gray area delimits the minimal hull of $\mathcal{C}$. Outside of this hull $n=0$ for all the plaquettes because otherwise we would need an infinite series of plaquettes with $n=1$, but we are interested only in the case of finite $\mathcal{L}$.

As example, let us consider the diagram $\mathcal{C}$ in Fig. 3. Our task is to find the values $n_{\triangle}$ which satisfy Eq. (3). A possible strategy is to find the values of the variables $n_{\triangle}$ starting from the topmost row and then to use Eq. (3) to solve the problem row by row moving downward. In order to see how the first

row can be determined, consider for instance the site $i$, which is the topmost left site belonging to the diagram $\mathcal{C}$: given that $\sum_{\triangle\!\!\triangle \in \mathcal{C} \cap \partial i} n_{\triangle\!\!\triangle} \equiv 1 \pmod 2$ and that no small plaquette can have $n_\triangle = 1$ outside the minimum hull shown in figure, we have to assign $n_\triangle = 1$ to the plaquette right below $i$; the same holds for all the topmost vertices in the diagram. All the small plaquettes in the first row which do not lie below a vertex of $\mathcal{C}$ are fixed to $n_\triangle = 0$, because they are outside the minimum hull of Fig.3. Once we have determined the values in the first row, we can find the values in the next and the following ones using Eq. (3) and the conditions on the variables $n_\triangle$ outside the hull: for instance, consider the site between $n_1, n_2 n_{,3}$ in the figure; for this vertex Eq. (3) reads $n_1 + n_2 + n_3 \equiv 0 \pmod 2$, which can be written as $n_3 \equiv n_1 + n_2 \pmod 2$. This clearly shows that the variables in the next row (the one of $n_3$) can be computed knowing the variables in the previous one $(n_1, n_2)$; to compute the variables near the boundary of the hull it is necessary to consider the fact that outside the hull $n_\triangle = 0$. In the end, when we compute the last row, either all the conditions are satisfied or we find some inconsistency; in the former situation we find the only diagram of small plaquettes that compensates the diagram $\mathcal{C}$, whereas in the latter we show that $\mathcal{C}$ cannot be closed.

It is also worth noting that such a simple formula as Eq. (3) leads to the appearance of fractal structures. Suppose, for example, that there is only one plaquette with $n_\triangle = 1$, with a triangular hull starting from below it; then, for each lattice site $j$ the equation reads $n_{\text{below j}} = n_{\text{above j,1}} + n_{\text{above j,2}}$, and whenever $n_{\text{above j,1}}$ lies outside the hull it is taken equal to 0 (the same holds for $n_{\text{above j,2}}$). These relations are the same that define the Pascal triangle (that of binomial coefficients) modulo 2, which is a fractal known as the *Sierpinski* triangle (Fig. 4). This fractal arises from other considerations: Garrahan and Newman ([6], and [11]) showed that $n$-spins correlation functions (w.r.t. the Newman-Moore model) can be written as

$$\langle s_{i_1} \cdots s_{i_n} \rangle = - \left(\tanh(\beta J)\right)^{\mathcal{N}_{i_1 \cdots i_n}} , \tag{4}$$

where $\mathcal{N}_{i_1 \cdots i_n}$ is computed in this way: below each vertex $i_k$ build a Pascal triangle modulo 2 – Sierpinski, – then sum (always modulo 2) the values appearing in the same places; $\mathcal{N}_{i_1 \cdots i_n}$ is the number of ones that are left. This number will usually be infinite: for instance, the single spin average (w.r.t. the NMM) is 0 at any finite temperature, since the number of odd numbers in a Pascal triangles is infinite.

The fact that given the variables $n_\triangle$ in a row we can compute the ones in the next row via Eq. (3) suggests that the problem of finding a set of spins (lying on the sublattice of the big plaquettes) with non-zero correlation function in the Newman-Moore model can be interestingly represented as a one dimensional *cellular automata* problem. A cellular automaton is a lattice model in which the value of each cell (1 or 0, *alive* or *dead*) at some time step

$t$ depends on the values of neighboring cells at $t-1$; the relation between our model and cellular automata is due to the fact that the dynamics of an automaton living in a one-dimensional space can be represented as a process on a two-dimensional space, in which the second coordinate corresponds to the time steps. Indeed, the same Eq. (3) (but on square lattices) defines what is called *Rule 90* or *Martin-Odlyzko-Wolfram* automaton or, for clear reasons, *Sierpinski* automaton, [9]; so, in terms of cellular automata, our problem can be recast as:

> Let $S_0(n) : 3\mathbb{Z} \to \{0,1\}$ be a function which is 1 if cell $n$ is alive at the initial time, 0 otherwise; let also $\{N_t(n)\}_{t>0}$ be a collection of functions from $\mathbb{Z}$ to $\{0,1\}$, and define the update rule as $S_{t+1}(0) = 1, S_{t+1}(n+1) = S_t(n) + S_t(n+1) + N_{t+1}(n+1) \pmod 2$. Then, is there any choice of the "perturbation" functions $\{N_t(n)\}$ that satisfies the following conditions?
>
> - $(n,t) \notin 3\mathbb{Z}^2 \implies N_t(n) = 0$,
> - $\{n \in \mathbb{Z} : S_t(n) = 1\} = \emptyset$ at some time $t$.

Therefore, the problem of finding closed diagrams in the perturbed NMM can be formulated as the search for a suitable perturbation in the dynamics of a cellular automaton.

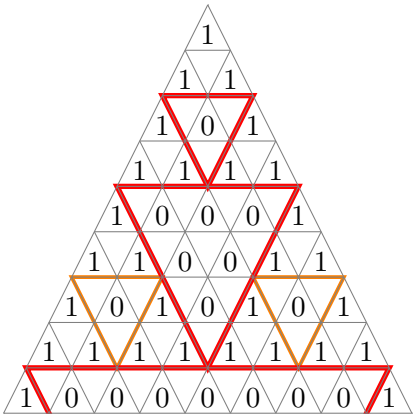


Figure 4: The Sierpinski triangle. In our problem, it is generated by (3) when there is a $n_\triangle = 1$, and provided that outside of the triangle $\{n_\triangle\}$ are constrained to be 0 (so that the borders have always $n = 1$). Note: the Sierpinski triangle appears because it is equal to the Pascal triangle (binomial coefficients) modulo 2 – i.e. it's parity. Indeed, the Pascal relation modulo 2 is $c_{n+1,k+1} \equiv c_{n,k} + c_{n,k+1} \pmod 2$ (compare it to (3)). Notice the periodicity of powers of 2: if the big plaquettes were of size 2 rather than 3, there would be many small closed diagrams!

## An interesting property of multispin correlation functions

Here we discuss a property of multispin correlation functions that may be useful to find the closure of big plaquette diagrams $\mathcal{C}$ in terms of small plaquettes. First of all, recall that saying that a set of spins $\mathcal{S} = \{s_i\}$ has correlation different from 0 means that $Z_\triangle^{-1} \cosh^{N_\triangle}(\beta J) \sum_{\{s\}} \prod_\triangle (1 + t s_{\triangle(1)} s_{\triangle(2)} s_{\triangle(3)}) \prod_{i \in \mathcal{S}} s_i \neq 0$ (for the sake of clarity we write explicitly

$\sigma_\triangle = s_{\triangle(1)}s_{\triangle(2)}s_{\triangle(3)}$). Rewriting the product as a sum over all diagrams of plaquettes $\mathcal{L}$, we can write the same condition as

$$\sum_{\{s\}}\sum_{\mathcal{L}} t^{|\mathcal{L}|}\prod_{\triangle\in\mathcal{L}} s_{\triangle(1)}s_{\triangle(2)}s_{\triangle(3)}\prod_{i\in\mathcal{S}} s_i \neq 0.$$

Clearly, the the product of spins in $\mathcal{S}$ has non-zero correlation if and only if one of the sets $\mathcal{L}$ is such that it compensates all the spins in $\mathcal{S}$, so that the term $\prod_{\triangle\in\mathcal{L}} s_{\triangle(1)}s_{\triangle(2)}s_{\triangle(3)}\prod_{i\in\mathcal{S}} s_i = 1$. Of course, the correlation is 0 if and only if there is no set $\mathcal{L}$ that can compensate the set $\mathcal{S}$.

Now, assume that $\mathcal{S}^\star$ is such a set of spins whose product has correlation different from 0; then, for any other set of spins $\mathcal{S}$ the following property holds:

$$\left\langle \prod_{i\in\mathcal{S}} s_i \right\rangle_\triangle = 0 \iff \left\langle \prod_{i\in\mathcal{S}} s_i \prod_{j\in\mathcal{S}^\star} s_j \right\rangle_\triangle = 0. \tag{5}$$

In what follows let $\mathcal{L}^\star$ be the set of plaquettes such that

$$\prod_{\triangle\in\mathcal{L}^\star} s_{\triangle(1)}s_{\triangle(2)}s_{\triangle(3)}\prod_{i\in\mathcal{S}^\star} s_i = 1. \tag{6}$$

$\Longleftarrow$ To prove this, first assume that the correlation of $\mathcal{S}$ is not 0: $\left\langle\prod_{i\in\mathcal{S}} s_i\right\rangle \neq 0$. This is equivqlent to sqy thqt there is a set of plaquettes $\mathcal{L}$ such that

$$\prod_{\triangle\in\mathcal{L}} s_{\triangle(1)}s_{\triangle(2)}s_{\triangle(3)}\prod_{i\in\mathcal{S}} s_i = 1. \tag{7}$$

It is straightforward to see that multiplying (6) and (7) we have

$$\prod_{\triangle\in\mathcal{T}} s_{\triangle(1)}s_{\triangle(2)}s_{\triangle(3)}\prod_{i\in\mathcal{S}} s_i \prod_{j\in\mathcal{S}^\star} s_j = 1.$$

where $\mathcal{T} = \mathcal{L}\ominus\mathcal{L}' = (\mathcal{L}\cup\mathcal{L}^\star)\setminus(\mathcal{L}\cap\mathcal{L}^\star)$ is the symmetric set difference and is such that $\prod_{\triangle\in\mathcal{T}}\sigma_\triangle = \prod_{\triangle\in\mathcal{L}}\sigma_\triangle\prod_{\triangle'\in\mathcal{L}^\star}\sigma_{\triangle'}$ (we have to use the symmetric difference instead of the union because for every plaquette in $\mathcal{L}\cap\mathcal{L}^\star$ $\sigma_\triangle^2 = 1$, hence double counting actually removes plaquettes from the product). For what we have said before, this last equation implies that $\left\langle\prod_{i\in\mathcal{S}} s_i\prod_{j\in\mathcal{S}^\star} s_j\right\rangle_\triangle \neq 0$.

$\Longrightarrow$ Consider now the other case, namely $\left\langle\prod_{i\in\mathcal{S}} s_i\right\rangle_\triangle = 0$; then, as said previously, for all sets $\mathcal{L}$ it must be that

$$\prod_{\triangle\in\mathcal{L}} s_{\triangle(1)}s_{\triangle(2)}s_{\triangle(3)}\prod_{i\in\mathcal{S}} s_i \neq 1 \tag{8}$$

and in particular the product still contains some spins that cannot be compensated; but then for sure multiplying by (6) – that is, multiply by 1, – the expression does not change:

$$\prod_{\triangle\in\mathcal{T}} s_{\triangle(1)}s_{\triangle(2)}s_{\triangle(3)} \prod_{i\in\mathcal{S}} s_i \prod_{j\in\mathcal{S}^\star} s_j \neq 1. \tag{9}$$

where $\mathcal{T} \equiv \mathcal{L} \ominus \mathcal{L}^\star$ as before. To conclude the proof we notice that the mapping $\mathcal{L} \to \mathcal{T} = \mathcal{L} \ominus \mathcal{L}^\star$ is a bijection from the set of all collections of plaquettes to itself, and therefore if (8) holds for all $\mathcal{L}$ than (9) does as well, and (5) is proven.

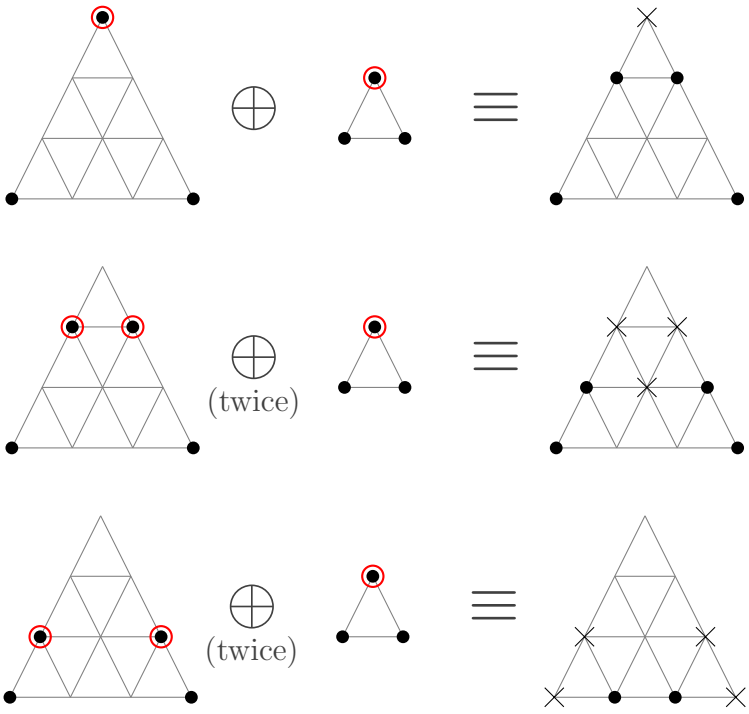


Figure 5: Visual representation of the game: multiplying (i.e. superimposing "modulo 2") a non-zero correlation set over another set of spins does not change the fact that the latter has a correlation equal to 0 or not.

This simple consideration allows us to translate the problem into another "game". The smallest set of spins with non zero correlation is the smallest triangle (i.e. the smallest cell of the triangular lattice); imagine superimposing the topmost vertex of this triangle on every topmost vertex of a set of big plaquettes, like in Fig. 5: repeating this scheme let us reduce the initial set to a set of points lying on one line only! Of course, it is very

easy to show that this set of points has non zero correlation if and only if it is the empty set (e.g. think of the Sierpinski triangle originating from the leftmost vertex: its left border will contain an infinite number of 1's, and hence the automaton will never die), and we *only* have to show that a set of spins belonging to big plaquettes can never be mapped into an empty set via this transformation.

## Partial traces and conclusions

The final attempt to demonstrate that arbitrary correlations of spins belonging to big plaquettes $\left\langle \prod_{\text{▲}\in\mathcal{C}} s_{\text{▲}(1)} s_{\text{▲}(2)} s_{\text{▲}(3)} \right\rangle_{\triangle}$ are zero is based on calculations with partial traces: the basic idea is to sum the partition function block by block, as in [12]. It is following this approach that we were able to prove that, contrary to our expectations, there is a finite diagram $\mathcal{C}$ such that $\left\langle \prod_{\text{▲}\in\mathcal{C}} s_{\text{▲}(1)} s_{\text{▲}(2)} s_{\text{▲}(3)} \right\rangle_{\triangle} \neq 0$. In the beginning we wanted to show that the high temperature expansion was $2^{N_\triangle} \cosh^{N_\triangle + N_\text{▲}}(\beta J)(1 + \text{corrections})$, where the correction terms are not an analytic function in the thermodynamic limit – if the system undergoes a transition at some temperature, – and vanish in the high temperature phase. In general, we can write the high temperature expansion as

$$Z = 2^{N_\triangle} \cosh^{N_\triangle + N_\text{▲}}(\beta J) \left( 1 + \sum_{n>0} c_n(N) \tanh^n(\beta J) \right). \qquad (10)$$

In the thermodynamic limit the non-analiticity due to a possible transition is entirely contained in the summation, and therefore if in the high temperature phase (i.e. for $\beta$ sufficiently small) the partition function is $\tilde{Z} = 2^{N_\triangle} \cosh^{N_\triangle + N_\text{▲}}(\beta J)$, the summation in Eq. (10) must sum to zero in this phase (in the limit $N \to \infty$); notice that given that every term is positive, each one must be 0 in the thermodynamic limit. In particular, for each $N$, let the lowest order term in $t \equiv \tanh(\beta J)$ with non-zero coefficient be $\gamma(N) t^{\alpha(N)}$ (we write explicitly the lattice size dependency – $N = N_\triangle$, for instance); then it follows that $\lim_{N\to\infty} \alpha(N) = \infty$. We will show that in fact there are only two possible cases: the partition function is *exactly* equal to $\tilde{Z}$ (but this cannot be true because it would not agree with the numerical simulations), or $\alpha(N)$ has to be bounded; furthermore, the coefficient $\gamma(N)$ (as all the coefficients) scales with $N$.

Imagine that we compute the partition function $\sum_{\{s\}} e^{\beta J (\sum_\triangle \sigma_\triangle + \sum_\text{▲} \sigma_\text{▲})} = \cosh^{N_\triangle + N_\text{▲}}(\beta J) \sum_{\{s\}} \prod_\triangle (1 + t\sigma_\triangle) \prod_\text{▲} (1 + t\sigma_\text{▲})$ — with $t = \tanh(\beta J)$, — on a finite square lattice (it actually is a rhombus, because the elementary cells are triangular), whose side length is a multiple of 3. Of course, apart from the prefactor $\cosh^{N_\triangle + N_\text{▲}}(\beta J)$ and a factor $2^{N_\text{spins}}$ due to the summation over the spins, the partition function is a polynomial $\mathcal{P}(t) = 1 + \sum_{n>0} c_n t^n$;

now assume that we do not sum over the spins on the last row, that is, we write

$$Z \propto \cosh^{N_{\triangle}+N_{\bigtriangleup}}(\beta J) \sum_{\{s\}'} \bar{\mathcal{P}}(t;\{s\}'), \tag{11}$$

where $\{s\}'$ refers to the spins in the last row and $\bar{\mathcal{P}}(t;\{s\}')$ is the polynomial in $t$ due to the sum over all the previous spins (the proportionality is due to the fact that we have omitted the power of two generated by the summation over spins). In particular, the terms in $\bar{\mathcal{P}}$ whose coefficients have some spin dependancy vanish when the sum in Eq. (11) is performed, and thus all the terms in $\mathcal{P}(t)$ are exactly those in $\bar{\mathcal{P}}$ without spin dependancy (but of course with a different coeffient, due to the sum); notice that the term 1 is present here, too. Now, assume that we compute the partition function relative to the same Hamiltonian, but on a lattice that is twice as big (in the vertical direction); given that the side length of the lattice was a multiple of 3, the last row of spins lied on the sublattice of the big plaquettes: this means that the interactions between the top and the bottom halves in the bigger lattice involve only spins lying on the bottom half and at most on the last row of the top one. Hence, we can write the new partition function just adding the suitable terms in Eq. (11) (and multiplying by the correct powers of 2 and $\cosh(\beta J)$):

$$Z_{\text{twice}} \propto \cosh^{2N_{\triangle}+2N_{\bigtriangleup}}(\beta J) \sum_{\{s\}'} \sum_{\substack{\{s\}\setminus\{s\}' \\ \text{bottom}}} \bar{\mathcal{P}}(t;\{s\}') \prod_{\substack{\triangle \\ \text{bottom}}} (1+t\sigma_{\triangle}) \prod_{\substack{\bigtriangleup \\ \text{bottom}}} (1+t\sigma_{\bigtriangleup}),$$

where $\{s\}'$ still refers to the last row of top half of the lattice, and "bottom" refers to plaquette terms due to the addition of lattice sites and, hence, plaquette interactions. Then, recalling that the polynomial $\bar{\mathcal{P}} \equiv 1 + t\bar{\bar{\mathcal{P}}}$ starts with 1, we can split the sum as

$$\begin{aligned} Z_{\text{twice}} \propto \cosh^{2N_{\triangle}+2N_{\bigtriangleup}}(\beta J) \Bigg( & \sum_{\substack{\{s\} \\ \text{bottom}}} \prod_{\substack{\triangle \\ \text{bottom}}} (1+t\sigma_{\triangle}) \prod_{\substack{\bigtriangleup \\ \text{bottom}}} (1+t\sigma_{\bigtriangleup}) + \\ & + \sum_{\{s\}'} \sum_{\substack{\{s\}\setminus\{s\}' \\ \text{bottom}}} \bar{\bar{\mathcal{P}}}(t;\{s\}') \prod_{\substack{\triangle \\ \text{bottom}}} (1+t\sigma_{\triangle}) \prod_{\substack{\bigtriangleup \\ \text{bottom}}} (1+t\sigma_{\bigtriangleup}) \Bigg). \end{aligned} \tag{12}$$

The key point now is to notice that the first term in Eq. (12), apart from factors relative to the size of this bigger lattice, is, by definition, the same as Eq. (11)! This is because the bottom half of the lattice has the same number of spins and interactions as the top half. Therefore, if $\bar{\mathcal{P}}$ has at least one term $t^{\alpha}$ without spin dependancy, this same term will be found also in the new partition function, namely $Z_{\text{twice}}$ (the only differences are

the powers of the factors 2 and $\cosh(\beta J)$); in particular, it follows that the minimum power of $t$ in $Z_{\text{twice}}$ is less than or equal to the minimum power of $t$ in $Z$ (because the second term in Eq. (12) might generate new powers of $t$ without spin dependancy, and these can in principle be of lower order; notice that being $\bar{\bar{\mathcal{P}}}$ made of positive terms, it cannot generate terms that somehow cancel $t^\alpha$)! In this case, therefore, the high temperature expansion of the partition function in the thermodynamic limit cannot be exactly equal to $\tilde{Z} = 2^{N_\triangle} \cosh^{N_\triangle + N_{\text{⧋}}}(\beta J)$. There is still the possibility that $\bar{\mathcal{P}}$ has no terms (except 1) without spin dependancy; in this case there are two possible scenarios: either the partition function is *exactly* equal to $\tilde{Z}$ (i.e. not only its high temperature expansion), or considering a bigger lattice we fall back in the previous case, that is $\bar{\mathcal{P}}$ has some term different from 1 without spin dependancy in its coefficient.

From the simulations we know that the partition function cannot be equal to $2^{N_\triangle} \cosh^{N_\triangle + N_{\text{⧋}}}(\beta J)$ without any correction (vanishing in the high temperature phase), because the low temperature behaviour is different. This means that the correct high temperature expansion is not equal to $\tilde{Z}$, but has some corrections; also, Eq. (2) implies that there must be some finite big plaquette diagram, and the natural question is what is the size of the smallest diagram. We already know that it cannot be too small; to find the actual value we performed a Monte Carlo simulation of the XORSAT problem defined by (3), and we looked for the ground states with a simulated annealing; the smallest diagram $\mathcal{C}$ found is made of 10 big plaquettes and can be closed with 54 small plaquettes (Fig. 6). Using the property of multispin correlations functions shown in Section 2 we verified that it actually had a correlation different from 0 (i.e. we were ablet to transform the diagram into the empty set). From (2) it follows that the corresponding correction to the partition function is proportional to $N_{\text{⧋}} \tanh^{64}(\beta J)$ (the coefficient is due to the fact that we can place this diagram anywhere in the lattice, and the exponent come from the 10 big plaquettes – $t^{|\mathcal{C}|}$ – and from the 54 plaquettes with $n_\triangle = 1$ needed to compensate the diagram).

The finding of such a closed diagram in the short range incommensurable triangle plaquette model allows us to also say something about the cellular automata problem explained in the section *Mapping to a XORSAT problem*. The answer to that problem is that we can certainly find the perturbation functions $\{N_t(n)\}_{t>0}$ such that the automaton dies at some finite time, whatever the initial conditions are. In particular, we can make it die at $t = 12$. To build these functions, imagine the space $(n, t)$ as a triangular lattice (e.g. the one in Fig. 1, with $n$ spanning the horizontal axis and $t$ spanning the top-right to bottom-left diagonal). Then, for any initial living cell $(n_0, 0)$ consider the set $P(n_0) = \{(n_0 + 3, 6),\ (n_0 + 3, 9),\ (n_0 + 6, 9),\ (n_0, 12),\ (n_0 + 12, 12)\}$, which correspond to the set of points of the

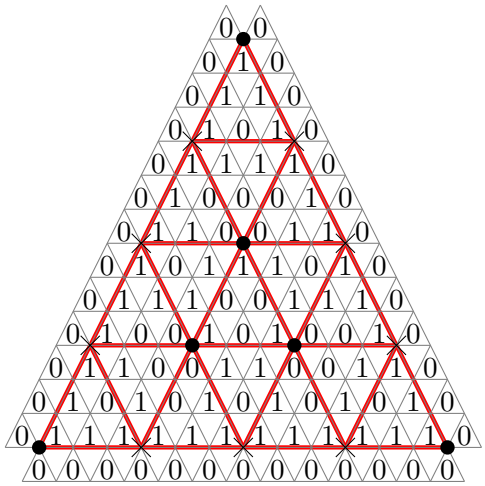

Figure 6: The smallest diagram with correlation different from 0. It is made of the 10 big plaquettes shown – red borders, – and due to the superposition of spins ($s^2 = 1$), it is equal to the correlation of the 6 circled spins in figure. Inside each plaquette is written the corresponding number $n_\triangle$, clearly proving that the cellular automaton dies in the last (bottom) row.

diagram in Fig. 6 if it were build with $(n_0, 0)$ as its topmost vertex; let then $P$ be the "multiplication" (superposition modulo 2) of all those sets (a point is in $P$ if and only if it belongs to an odd number of the sets $\{P(n_0)\}_{n_0}$). It is easy to see that if we choose $N_t(n) = 1$ for the points $(n, t) \in P(\subset 3\mathbb{Z}^2$ because $n_0 \in 3\mathbb{Z}$ by hypothesis) and 0 otherwise, then the cellular automaton dies at $t = 12$.

# 3 Random long range triangular plaquette model

In this section we describe another model that we have been studying. We consider the Newman-Moore model with the addition of a long range perturbation: the lattice is the same as the NMM, but we add 3-spin plaquette interactions between triplets of spins chosen at random among the whole set; the Hamiltonian is formally similar to that of the previous model,

$$H_0 + \varepsilon H_1 = -J \sum_{\triangle} s_{\triangle(i)} s_{\triangle(j)} s_{\triangle(k)} - \varepsilon J \sum_{\blacktriangle} s_{\blacktriangle(i)} s_{\blacktriangle(j)} s_{\blacktriangle(k)}, \qquad (13)$$

but the second sum is over the random, long range plaquettes (the first one is the usual NMM Hamiltonian). While the high temperature phase in the Newman-Moore model is different from the one in the short range triangular plaquette model, we are motivated to believe that the situation may be different for the long range Hamiltonian $H_0 + \varepsilon H_1$. We think that this model is *marginal* in the sense that as long as $\varepsilon \neq 0$, whatever the value, the system has a glass transition at a temperature $T^\star(\varepsilon) > 0$, whereas for $\varepsilon = 0$ the transition is at zero temperature and the thermodynamics is trivial. We expect the glass transition to happen at finite temperature for the analogy of plaquette models with XORSAT problems; as already said, these problems consist in assigning values to $N$ binary variables, such that they satisfy $M$ linear equations modulo 2. They have always solution for $N = M$, and this is the case corresponding to the NMM, but for $M > N$ it might not have any solution at all! The analogy between the two problems is due to the fact that the low temperature excitations of plaquette models obey modular equations similar to (3), but on spin rather than plaquette variables.

We study the dynamics of the system either numerically and also analitically by approximating the regular triangular lattice with long range interactions as a model on a Bethe lattice with a topology as close as possible (i.e. same distribution of vertex degrees and same distribution of long range plaquettes among the spins). In the following chapter we present the Bethe approximation and the procedure used to sample the correct statistical properties, and we will also make a comparison with the simulations: these have been done on a lattice of 64x64 plaquettes with 400 additional long range interactions, with coupling constants $J = \varepsilon J = 1$, with a Monte Carlo algorithm based on a single spin flip dynamics. We perform an annealing, both starting from a system prepared in a paramagnetic phase (gradually led towards lower temperatures) and from one prepared in the ferromagnetic ground state (gradually led towards higher temperatures); in both cases the temperature steps are $\delta T = 0.04$, and the MC steps are $10^6$ or $10^7$ according to whether $T > 0.72$ or $T < 0.72$.

# 4 Bethe lattice approximation

We studied a version of the previous model on a Bethe lattice, with the idea that it would have been easier to study the glassy behavior. The major advantage of using trees is that algorithms as Belief Propagation (BP) are exact and converge rapidly (in a time that scales linearly with the dimension of the system). BP is a message passing algorithm and it can be used to compute marginal distributions, exactly on trees and approximately on graphs with loops, [10]. In our model, the corresponding factor graph is a tree whose vertices are spin variables $\{s_i\}_i$ and whose action nodes are the plaquettes $\{\sigma_\triangle\}_\triangle$; the joint distribution of the spin variables is given by the canonical Boltzmann weight, $\mathbb{P}(\mathbf{s};\beta) = Z^{-1}e^{-\beta H(\mathbf{s})}$, with $H(\mathbf{s}) = -J\sum_\triangle s_{\triangle(1)}s_{\triangle(2)}s_{\triangle(3)} - J'\sum_\blacktriangle s_{\blacktriangle(1)}s_{\blacktriangle(2)}s_{\blacktriangle(3)}$ (in the following $J = J'$ and $\triangle$ will denote both short range and long range plaquettes). The functions which are updated by the algorithm are the messages associated with each edge of the factor graph, i.e. $\nu_{i\to\triangle}(s_i)$, $\tilde{\nu}_{\triangle\to i}(s_i)$; these functions, which computationally speaking are simple variables, being normalized two-valued functions, are the marginal probability distributions computed removing specific parts of the graph. For simplicity we will use the variables $h_{i\to\triangle}$, $u_{\triangle\to i}$ such that $\nu_{i\to\triangle}(s_i) = \frac{e^{\beta h_{i\to\triangle}s_i}}{2\cosh(\beta h_{i\to\triangle})}$, $\tilde{\nu}_{\triangle\to i}(s_i) = \frac{e^{\beta u_{\triangle\to i}s_i}}{2\cosh(\beta u_{\triangle\to s_i})}$: in terms of these variables the BP equations become

$$\begin{aligned} h_{i\to\triangle} &= \sum_{\triangle'\in\partial i\setminus\triangle} u_{\triangle'\to i}, \\ \tanh(u_{\triangle\to i}) &= \tanh(\beta J)\prod_{j\in\partial\triangle\setminus i}\tanh\left(\beta h_{j\to\triangle}\right). \end{aligned} \tag{14}$$

To find the solution (fixed point) to these equations we compute the variables $\{h^{(t+1)}_{i\to\triangle}, u^{(t+1)}_{\triangle\to i}\}$ in function of $\{h^{(t)}_{i\to\triangle}, u^{(t)}_{\triangle\to i}\}$, starting with some initial conditions; on trees, this procedure always converge. Of course, we can make a few assumptions on these messages, as suggested by symmetries. We assume that messages concerning edges with the same type of neighbors are equal, e.g. $h_{i\to\triangle}$ is not different for all the edges $(i,\triangle)$, but only for those embedded in sub-trees which are locally different. Now, being this Bethe lattice an approximation to our plaquette model with long range interactions, its factor graph has two possible action nodes: one is the lattice plaquette, and the other is the extra (long range) plaquette; hence, a spin could have 3 or 4 neighboring action nodes, according to whether a long range plaquette had been added to it or not.

Therefore there are 5 possible messages (shown in Fig. 7): from a spin belonging to 3 (lattice) plaquettes to one of its plaquettes $\left(h^{(3)}_{i\to L}\right)$, from a spin belonging to 4 plaquettes (one of which must be long range) to one of its lattice plaquettes $\left(h^{(4)}_{i\to L}\right)$ or to its extra plaquette $\left(h^{(4)}_{i\to X}\right)$, and from a lattice or long range plaquette to one of its spins $(u_{L\to i},\ u_{X\to i})$ ($i,\ L,\ X$ in the subscripts do not refer to particular nodes). Then, the BP equations for these messages are ($L',\ L'',\ L''',\ X',\ j,\ k$ refer to the other plaquettes and spins neighboring the relevant node):

$$\begin{aligned}
&h^{(3)}_{i\to L} = u_{L'\to i} + u_{L''\to i},\\
&h^{(4)}_{i\to L} = u_{L'\to i} + u_{L''\to i} + u_{X'\to i},\\
&h^{(4)}_{i\to X} = u_{L'\to i} + u_{L''\to i} + u_{L'''\to i},\\
&\tanh(u_{L\to i}) = \tanh(\beta J)\tanh\left(\beta h^{(3,4)}_{j\to L}\right)\tanh\left(\beta h^{(3,4)}_{k\to L}\right),\\
&\tanh(u_{X\to i}) = \tanh(\beta J)\tanh\left(\beta h^{(4)}_{j\to X}\right)\tanh\left(\beta h^{(4)}_{k\to X}\right).
\end{aligned} \tag{15}$$

(As before, to find the fixed point we use a recurrent relation). The equation for $u_{L\to i}$ is particular because the messages coming from its neighboring spins can either be of type $h^{(3)}_{i\to L}$ or $h^{(4)}_{i\to L}$, and thus we have to average over them with the suitable probability. Given that in the long range model we added $\alpha N$ long range plaquettes ($N$ being the number of short range plaquettes), the probability that a spin has 4 neighboring plaquettes (rather than 3) is $3\alpha$, because every plaquette is connected to 3 spins and hence $3\alpha N$ spins are connected to one long range plaquette; now, because of the involved symmetry, the probability of picking an edge of type $h^{(4)}_{i\to L}$ is $\frac{3}{4}$ times the probability of picking a spin with four plaquettes. Therefore, the probability of picking an edge $h^{(4)}_{i\to L}$ rather than $h^{(3)}_{i\to L}$ is $\frac{3\alpha\cdot\frac{3}{4}}{3\alpha\cdot\frac{3}{4}+1-3\alpha} = \frac{9\alpha}{4-3\alpha}$.

Instead of actually building a Bethe lattice in a simulation, run the Belief Propagation (BP) equations, and then average over an ensemble of trees, we perform a population dynamics of distributions; rather than writing recurrent relations for the single message variables $h, u$, we use distributions of messages (one per type), sample from them and update them with BP equations.

First, we build the corresponding distributions $P_{h^{(3)}_{i\to L}}$, $P_{h^{(4)}_{i\to X}}$, $P_{h^{(4)}_{i\to L}}$, $Q_{u_{X\to i}}$, $Q_{u_{L\to i}}$; initially these are uniformly $+1$ or random Gaussian to find the ferromagnetic and paramagnetic solutions, respectively. Then, we up-

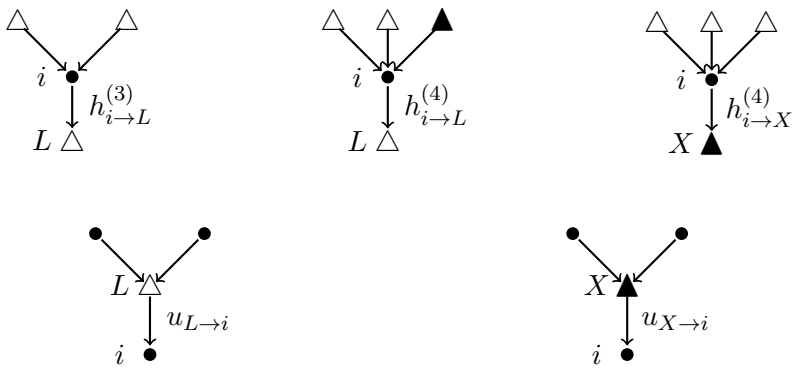


Figure 7: All the different messages we can find the the Bethe lattice. Black plaquettes are "long range".

date them with the following equations:

$$
\begin{aligned}
P_{h^{(3)}_{i\to L}}(h) &= \int \mathrm{d}Q_{u_{L\to i}}(u)\ \mathrm{d}Q_{u_{L\to i}}(v)\ \delta(h-(u+v)),\\
P_{h^{(4)}_{i\to L}}(h) &= \int \mathrm{d}Q_{u_{L\to i}}(u)\ \mathrm{d}Q_{u_{L\to i}}(v)\ \mathrm{d}Q_{u_{X\to i}}(w)\ \delta(h-(u+v+w)),\\
P_{h^{(4)}_{i\to X}}(h) &= \int \mathrm{d}Q_{u_{L\to i}}(u)\ \mathrm{d}Q_{u_{L\to i}}(v)\ \mathrm{d}Q_{u_{L\to i}}(w)\ \delta(h-(u+v+w)), \quad (16)\\
Q_{u_{L\to i}}(u) &= \int \mathrm{d}\tilde{P}(h)\ \mathrm{d}\tilde{P}(g)\ \delta\left(u-\mathcal{U}(h,g;\beta,J)\right),\\
Q_{u_{X\to i}}(u) &= \int \mathrm{d}P_{h^{(4)}_{i\to L}}(h)\ \mathrm{d}P_{h^{(4)}_{i\to L}}(g)\ \delta\left(u-\mathcal{U}(h,g;\beta,J)\right).
\end{aligned}
$$

where $\mathcal{U}(h,g;\beta,J) = \tanh^{-1}\left(\tanh(\beta J)\tanh(\beta h)\tanh(\beta g)\right)$, and $\tilde{P}(h)$ has to be chosen, at each run of the iterative procedure, equal to $P_{h^{(4)}_{i\to L}}(h)$ with probability $a \equiv \frac{9\alpha}{4-3\alpha}$ and equal to $P_{h^{(3)}_{i\to X}}(h)$ otherwise.

The corresponding algorithm has been implemented in the following way (at fixed temperature $\beta$ and coupling $J$):

- First, we define the five arrays $\mathtt{P}_{h^{(3)}_{i\to L}}$, $\mathtt{P}_{h^{(4)}_{i\to X}}$, $\mathtt{P}_{h^{(4)}_{i\to L}}$, $\mathtt{Q}_{u_{L\to i}}$, $\mathtt{Q}_{u_{X\to i}}$, each with 10000 elements, distributed uniformly or according to a Gaussian law to find both ferromagnetic and paramagnetic solutions.
- Just for example, we consider only the array $\mathtt{Q}_{u_{X\to i}}$. In a loop, at each step we update the array, randomly and asynchronously: we sample three uniform random numbers from 0 to 10000, $n_1, n_2, n_3$, and compute $\mathtt{Q}_{u_{X\to i}}[n_1] = \mathcal{U}\left(\mathtt{P}_{h^{(4)}_{i\to X}}[n_2], \mathtt{P}_{h^{(4)}_{i\to X}}[n_3]; \beta, J\right)$. The update for the other distributions is performed in the same way, with the exception of $\mathtt{Q}_{u_{L\to i}} = \mathcal{U}(\mathtt{P}[n_2], \mathtt{P}[n_3]; \beta, J)$, where $\mathtt{P}$ is set equal to $\mathtt{P}_{h^{(4)}_{i\to X}}(h)$ with

probability $a$ and to $\mathtt{P}_{h^{(3)}_{i\to X}}(h)$ otherwise, independently for each argument.

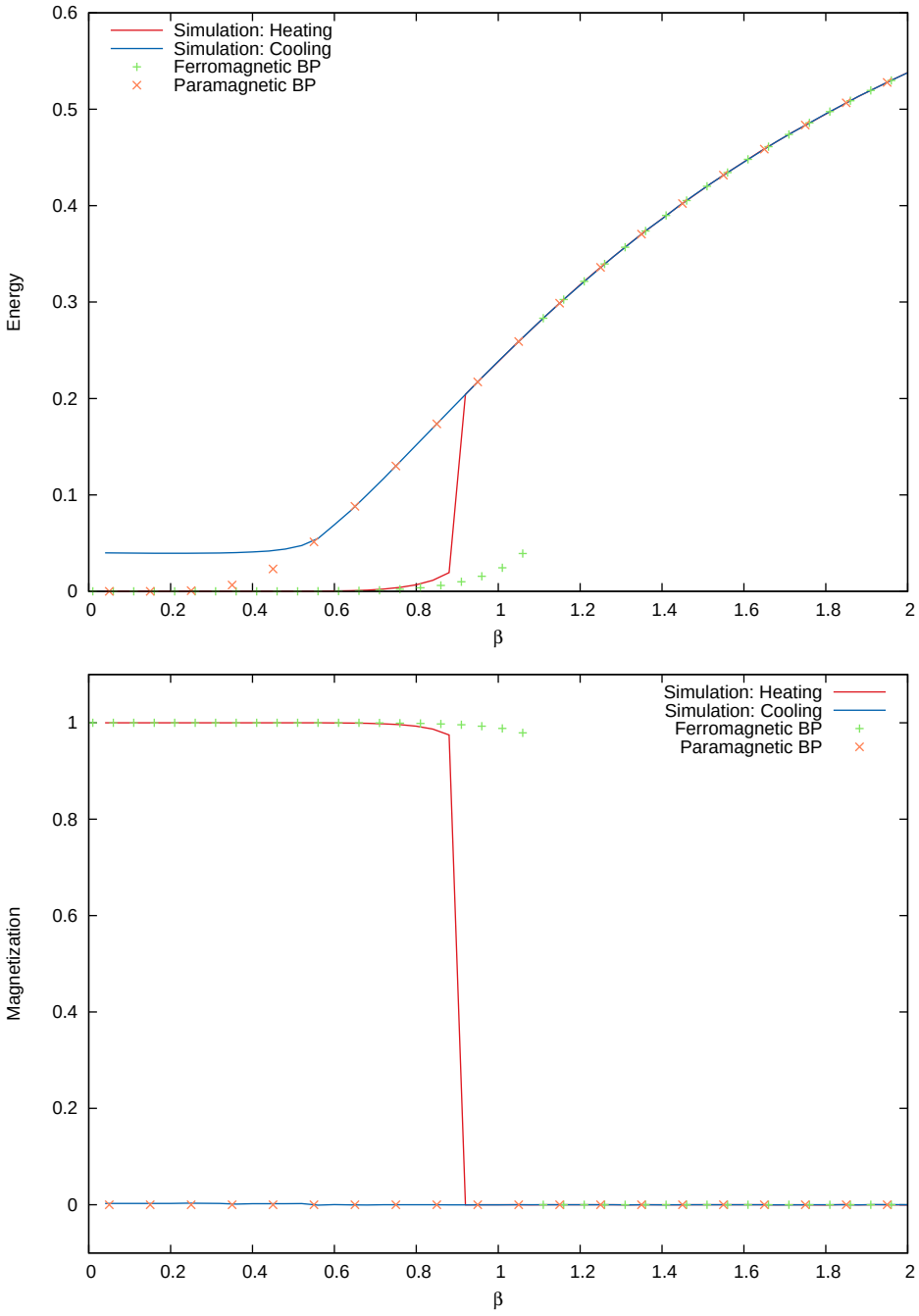


Figure 8: Energy and magnetization, in Bethe lattice approximation and actual simulations – the annealing has been done in both directions. ($J = 1,\ T = \frac{1}{\beta}$).

- Once the iterations converge to a fixed value, we measure the average magnetization and energy. For a given edge $(i, \triangle)$, its magnetization is $\tanh\left(\beta\left(h_{i\to\triangle} + u_{\triangle\to i}\right)\right)$, so we have to average over the distribution of edge/message types, which depends on the probability $p = \frac{\alpha}{1+\alpha}$ of picking at random a long range plaquette, rather than a short range one. Thus, with probability $p$ the magnetization is $\tanh\left(\beta\left(\mathtt{P}_{h^{(4)}_{i\to X}}[n_1] + \mathtt{Q}_{u_{X\to i}}[n_2]\right)\right)$, whereas with probability $1-p$ $\tanh\left(\beta\left(\mathtt{P}[n_1] + \mathtt{Q}_{u_{L\to i}}[n_2]\right)\right)$, where $\mathtt{P}, n1, n2$ are as before.

- The energy is a computed analogously; the contribution of any plaquette $\triangle$, either long range or short range, is given by

$$\frac{\tanh(\beta J) + \tanh(\beta h_1)\tanh(\beta h_2)\tanh(\beta h_3)}{1 + \tanh(\beta J)\tanh(\beta h_1)\tanh(\beta h_2)\tanh(\beta h_3)},$$

  where $h_1, h_2, h_3$ are the messages incoming from its neighboring spins. Therefore, with probability $p$ they are all extracted from $\mathtt{P}_{h^{(4)}_{i\to X}}$ and with probability $1-p$ each of them has to be sampled independently from $\mathtt{P}_{h^{(3)}_{i\to L}}$ (with probability $1-a$) or $\mathtt{P}_{h^{(4)}_{i\to L}}$ (with probability $a$).

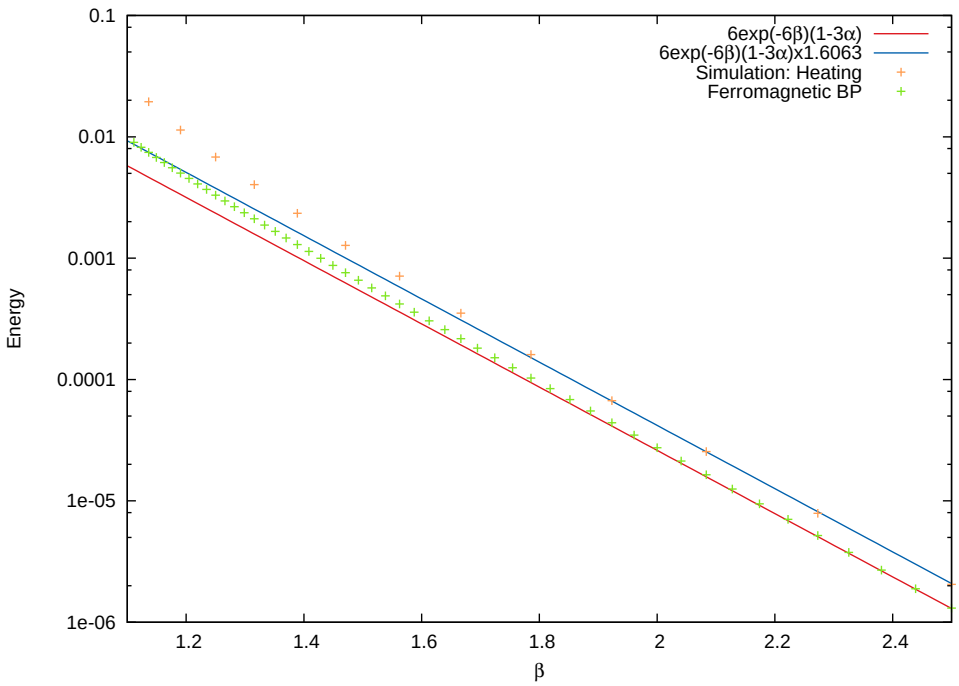


Figure 9: Energy of the two models in log scale for sufficiently high values of $\beta$.

In Fig. 8 are shown the plots of energy and magnetization found with this Bethe lattice approach, compared with the actual data from a simulation on a 64x64 lattice, with $J = 1$. We see that the two systems have different low temperature phases, and hence the Bethe lattice approximation does not actually hold; the reason of this can be understood looking at the low temperature expansion of the energy. The first term of this expansion is the contribution given by the smallest excitations above the ground state: in the Bethe lattice, a single spin flip changes the energy by ($J = 1$ in the following) $\Delta H = 2n$ where $n$ is the number of neighboring plaquettes; then, of course, the smallest excitation is given by spins without any long range plaquette and it is equal to $\Delta H = 6$. Keeping in mind that the fraction of these spins is $1 - 3\alpha$, we can say that the first term in the expansion is $6e^{-6\beta}(1 - 3\alpha)$, and in Fig. 9 it is easily seen that this is indeed the case. On the other hand, the same minimal excitation can be achieved in more ways in the lattice with long range interactions (two of such ways are shown in Fig. 10); with a fit we find that the combinatorial coefficient in this case is not $1 - 3\alpha$, but $\approx 1.6063(1 - 3\alpha)$ (notice that $(1 - 3\alpha) + (1 - 3\alpha)^3 \approx 1.0605 < 1.6063(1 - 3\alpha) \approx 1.1357$, therefore there must be other lowest energy excitations). Therefore, the Bethe approximation is not valid and cannot be used to study the transition of the lattice model with long range interactions.

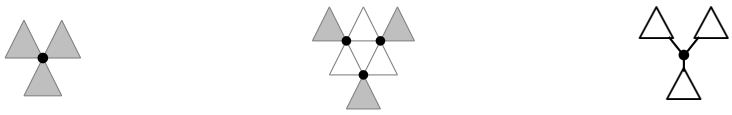

Figure 10: The first two diagrams are two of the smallest excitations in the lattice model (their combinatorial factors are $1 - 3\alpha$, $(1 - 3\alpha)^3$); the last diagram is the only smallest excitation of the Bethe lattice model (its combinatorial factor is $1 - 3\alpha$). In all cases flipping the central spin(s) gives $\Delta H = 6$; in the second case – the one with 3 spins, – the central, white plaquettes do not contribute because $\sigma = s_1(-s_2)(-s_3) = s_1 s_2 s_3$.

# 5 Conclusions

As shown in [4, 6, 11], quenched disorder is not a strict requirement to have a glassy behavior. Indeed, this can be found in ordered short range plaquette models; it is remarkable that while they are paradigmatic examples of the "dynamic facilitation" scenario, the same models in mean field approximation (for instance the $p$-spin model) display a thermodynamic glass transition at finite temperature, suggesting that perhaps the description of glass formation as a thermodynamic transition or as a purely dynamic process may be not contradictory, but rather complementary descriptions of the same kind of physics (note that explicit mappings between "thermodynamic" spin glasses and KCMs have been studied e.g. in [3, 8]).

In this report we studied different kinds of perturbations applied to the two-dimensional Newman-Moore model, as we think that they may lead to interesting behaviors – a finite temperature glass transition, for instance. To be more complete, these studies should consider also some other approaches to be: first of all, it might be interesting to increase the dimensionality of the lattices in both the long range random triangular plaquette model (LRRTPM) and in the incommensurable triangular plaquette model (ITPM), as that would increase the frustration of the system (i.e. the number of conflicting interactions per spin) and therefore the glassiness as well – we should use either "planar" (3-spin) or "tetrahedral" (4-spin) plaquette interactions. Another issue that has not been addressed in the LRRTPM is whether there are substantial changes as one varies $(\alpha, \varepsilon)$, $\alpha$ being the fraction of long range plaquettes added to the NMM, and $\varepsilon$ being the relative strength of their couplings; we know that the glass transition is at zero temperature for $\varepsilon = 0$ and we expect it to be at a higher temperature for $\varepsilon \neq 0$, but we do not know amuch about the importance of $\alpha$. For what concerns the IPTM, on the other hand, we still have to study the single defect low temperature dynamics. All these points will be studied in a further research.

**Acknowledgements**

I would like to thank Silvio Franz and Giacomo Gradenigo for having taught me so much during this internship. Also, I thank Gino, Riccardo, Silvia, Eiji, Fabio and my family for their support, and, of course, Artù, Alessandro, Alessio, Marco and all my friends who are far away.

# 6 Bibliography


[1] R. J. Baxter. *Exactly solved models in statistical mechanics*. Dover, 2007.

[2] T. Castellani and A. Cavagna. Spin glass theory for pedestrians. *J. Stat. Mech. P05012*, 2005.

[3] L. Foini, F. Krzakala, and F. Zamponi. On the relation between kinetically constrained models of glass dynamics and the random first-order transition theory. *J. Stat. Mech. P06013*, 2012.

[4] S. Franz, M. Mézard, F. Ricci-Tersenghi, M. Weigt, and R. Zecchina. A ferromagnet with a glass transition. *Europhys. Lett. 55, 465*, 2001.

[5] J. P. Garrahan. Glassiness through the emergence of effective dynamical constraints in interacting systems. *Journal of Physics Condensed Matter*, 2001.

[6] J. P. Garrahan and M. E. J. Newman. Glassiness and constrained dynamics of a short-range non-disordered spin model. *Phys. Rev. E 62, 7670-7678*, 2000.

[7] J. P. Garrahan, P. Sollich, and C. Toninelli. *Kinetically constrained models*. Oxford University Press, 2011.

[8] H. Jia, C. Moore, and B. Selman. From spin glasses to hard satisfiable formulas. 2012.

[9] O. Martin, A. M. Odlyzko, and S. Wolfram. Algebraic properties of cellular automata. *Commun. Math. Phys. 93, 219-258*, 1984.

[10] M. Mézard and A. Montanari. *Information, Physics, and Computation*. Oxford University Press, 2009.

[11] M. E. J. Newman and C. Moore. Glassy dynamics and aging in an exactly solvable spin model. *Phys. Rev. E 60, 5068-5072*, 1999.

[12] C. Yamaguchi. Static exact solutions of a spin model exhibiting glassy dynamics. *arXiv:1012.5651*, 2012.